Advancing Mistuning Identification and Dynamic Modeling of Blisks Through Blade Detuning Tests

Advancing Mistuning Identification and Dynamic Modeling of Blisks through Blade Detuning Tests

Biao Zhou, * Ankang Li, †
Nanjing University of Aeronautics and Astronautics, Nanjing, 210016, China

Giuseppe Battiato ‡ Teresa M. Berruti §
Politecnico di Torino, Torino, 10129, Italy

Blisks extensively used in the advanced aero-engines are vulnerable to vibration problems, due to the high sensitivity of the blisk's forced response to blade mistuning. This paper proposes an emerging mistuning identification technique based on Blade Detuning Tests (BDTID) for predictive dynamic modeling of blisks. The conventional frequency-mistuning modeling approaches relying on blade mistuning identification by reduced-order model techniques and modal test data of the full blisk are also adopted to construct different mistuned models of a blisk test piece for comparison purposes. A complete assessment of these blisk models is achieved through the forced response tests in a stationary traveling wave excitation test rig. The BDTID consists of blade detuning tests followed by a correction procedure. The detuning tests enable to approximately evaluate the 'blade-alone' frequencies through blade-by-blade impact testing in combination with a mass detuning mechanism. The correction procedure is able to evaluate the detuning test quality by the quantification of the residual inter-blade coupling due to mass detuning. More importantly, a robustness investigation demonstrates that this procedure is able to capture the 'true' blade mistuning even in case of poor blade detuning test quality. The resultant mistuned blisk model exhibits high accuracy in the modal correlation and forced response validation results. Compared with the conventional methods, BDTID takes advantage of easy implementation with less experimental effort and proved robust performance. It is therefore recommended for blade mistuning identification and predictive blisk dynamic modeling in a wide variety of scenarios.

Nomenclature

N = number of blades

*Associate Professor, College of Energy and Power Engineering, 29 Yudao St., biao.zhou@nuaa.edu.cn.
†Master student, College of Energy and Power Engineering, 29 Yudao St., liankang@nuaa.edu.cn.
‡Assistant Professor, Dipartimento di Ingegneria Meccanica e Aerospaziale, Corso Duca degli Abruzzi 24, giuseppe.battiato@polito.it.
§Professor, Dipartimento di Ingegneria Meccanica e Aerospaziale, Corso Duca degli Abruzzi 24, teresa.berruti@polito.it.

$\mathbf{I}$ = identity matrix

$\mathbf{Q}$ = a matrix of modal participation factors

p = a vector of modal coordinates

$\boldsymbol{\beta}$ = a vector of weighting factors

$\boldsymbol{\Delta}$ = a circulant matrix of blade modulus mistuning values

${}^{f}\delta$ = blade frequency mistuning pattern

${}^{E}\delta$ = blade modulus mistuning pattern

$\boldsymbol{\lambda}$ = a vector of tuned system frequencies

$\boldsymbol{\lambda}^{\delta,\mathrm{cb}}$ = a vector of cantilevered-blade eigenvalue deviations

$\boldsymbol{\kappa}^{\delta}$ = a matrix of cantilevered-blade eigenvalue deviations

$\boldsymbol{\Phi}^{\circ}$ = modal matrix of a tuned blisk

$\boldsymbol{\phi}$ = a mistuned blisk mode

$\boldsymbol{\Psi}$ = a circulant matrix of influence coefficients

$\boldsymbol{\psi}$ = a vector of influence coefficients

$\boldsymbol{\Omega}^{\circ}$ = a diagonal matrix of tuned blisk frequencies

$\bar{\boldsymbol{\Omega}}$ = a matrix of DFT of sector frequency deviations

ω = mistuned blisk frequency

$\bar{\boldsymbol{\omega}}$ = a vector of DFT of the sector frequency deviation

Subscripts

m = blade-alone mode order

j = generic variable

ref = reference

I. Introduction

A blisk is one-piece integral component of aero-engine modules consisting of a series of blades coupled by a rotor disk. Blisks have soared in popularity in the advanced aero-engine due to the benefits they contribute to the improved engine performance, driving efficiency, and reduced engine weight.

Although a blisk in the nominal design has identical blades, there are always random, inevitable deviations in geometry shapes/physical properties among the blades, which is referred as mistuning. Even though blade mistuning is typically small, it has a profound effect on the system dynamics of blisks. Mode localization and excessive blade vibration level are commonly observed for the blisks under rig/engine tests. In order to gain an exact understanding of the structural dynamics of a given blisk, it is important to experimentally identify the blade mistuning pattern actually

present in the blisk for the purpose of predictive blisk modeling.

A common basis of the widely spread dynamic modeling strategies of mistuned blisks is to interpret blade mistuning as the deviation of 'blade-alone' frequencies (or sector frequencies) from the nominal design. This is realized by applying small perturbations either to the stiffness matrix or, equivalently, to the mass matrix of each individual blade [1, 2]. Blade mistuning identification conventionally exploits an inverse form of Reduced-Order Model (ROM), specifically for blisks with frequency mistuning, and requires the measured modal information of the full blisk as input data. The identification procedure varies depending on the ROM adopted in the identification process, e.g., the Fundamental Mistuning Model IDentification (FMMID) method [3] and Component Mode Mistuning IDentification (CMMID) method [4, 5]. In essence, the blade mistuning identification methods formulated as inverse problems, are prone to the input error of the measured full-blisk mode shapes. It thus requires intensive experimental efforts to accurately retrieve the modal properties of the whole mistuned blisk [6–10].

Alternatively, the 'blade-alone' frequencies in a blisk can be approximately evaluated by the Blade Detuning Tests (BDT). The BDTs consist of blade-by-blade impact testing of a blisk with detuning mass purposefully attached on all the blades except the one under test. The detuning mass is used to decouple the single blade vibration from the full blisk by suppressing the inter-blade coupling within the blisk [11]. Blade mistuning patterns are furthered determined as 'blade-alone' frequency variations in a direct way. Nevertheless, it has been aware that the detuning masses can not completely eliminate the inter-blade coupling. The residual inter-blade coupling might lead to inaccurate blade mistuning pattern directly evaluated from the blade detuning test results [12, 13]. An influence coefficient method was conceptually proposed to quantify the residual inter-blade coupling for the purpose of accurate mistuning identification [14]. The so-called 'cyclic modeling error' was further taken into account in a continuous research in order to eliminate the arbitrariness of the identified mistuning pattern [15]. Inspired by the concept of influence coefficients, nevertheless, stemming from a fundamentally different assumption, a new blade mistuning identification procedure based on the correction of blade detuning test results (the term 'BDTID' will be used throughout this paper for this procedure) was recently proposed by the authors in order to capture the 'true' blade-alone mistuning with improved accuracy [16]. Compared with the conventional identification methods relying on ROM techniques and the global modal tests for the whole blisk, the emerging identification methods based on blade detuning tests take advantage of simple implementation with less experimental effort. This feature makes it appealing in the identification practice.

In spite of the living research interest, no attempt was made to verify the blade mistuning identified based on blade detuning tests and accordingly the resultant mistuned blisk model for the forced response prediction. In fact, due to the high sensitivity of the blisk's forced response to blade mistuning, the complete assessment of the mistuned blisk models can only be achieved through forced response tests under engine order-like excitation. In addition, it has been revealed that a number of factors, such as the quantity and position of detuning mass on the blades, as well as the inherent dynamic characteristics of the blisk, etc, could have an impact on the blade detuning test quality and therefore

the accuracy of identified mistuning patterns. Effectiveness and robustness of this promising mistuning identification technique deserves more in-depth research efforts.

This paper presents a comprehensive study and a critical analysis in order to advance the existing mistuning identification and predictive dynamic modeling capability of mistuned blisks. Specifically, three dynamic models of an integrally manufactured blisk test piece will be constructed and verified against the modal test data: (1) Model-FMMID; (2) Model-CMMID; (3) Model-BDTID. As indicated by the model names, blade mistuning is identified by different methods respectively. For instance, 'Model-BDTID' denotes a mistuned blisk model with the blade mistuning identified by the BDTID method, and so forth. Benefiting from the test capability of a well-developed stationary traveling wave excitation rig, forced response of the blisk under engine order-like excitation typically occurring in the aero-engine can be experimentally simulated and measured. Accordingly, predictive performance of the mistuned blisk models in terms of forced response can be examined.

The objective of this research is twofold. On the one hand, performance of the emerging BDTID method for predictive blisk dynamic modeling will be assessed and compared with the conventional blade mistuning identification methods requiring the global blisk mode shape measurements, i.e. FMMID and CMMID. On the other hand, robustness of the BDTID method in case of different blade detuning test quality will be investigated in depth. This is of significant relevance in the sense that the turbomachinery community is eager for a reliable method in order to accurately identify blade mistuning for safe operation of blisks within the scope of rig/engine tests [17–20].

This paper is organized as follows: Sec. II illustrates the test campaigns and the different modeling methodologies for the given blisk test piece; the resultant mistuned blisk models are verified against the modal test data in Sec. III; the blisk is then subjected to forced response tests in a stationary traveling wave excitation test rig. Prediction capabilities of the aforementioned mistuned blisk models are finally assessed and validated in Sec. IV.

II. Dynamic Modeling for the Mistuned Blisk

Fig. 1a shows the integrally manufactured blisk test piece mounted onto a stationary traveling wave excitation test rig, which will be described later on. The blisk is made of steel with nickel plated, and consists of $N = 12$ nominally identical sectors with simplified geometric shape. The disk center is clamped by bolts with controlled torque. In the nominal finite element sector model presented in Fig. 1b, the detailed geometry features around the center are neglected for simplicity.

The dynamic characteristics of the blisk in its nominal design are represented by the numerical frequency vs nodal diameter diagram in Fig. 2. In addition, the coupling index (CI) [21], i.e. the quantitative measurement of the inter-blade coupling, is displayed for each blisk mode on the same plot. The mode-dependent coupling index takes a value from 0% to 100%. CI = 0% represents a purely blade-alone mode with rigid disk, i.e. no inter-blade coupling exists. CI close to 100% denotes a high disk participation in the blisk mode and thus the inter-blade coupling nearly arrives at full

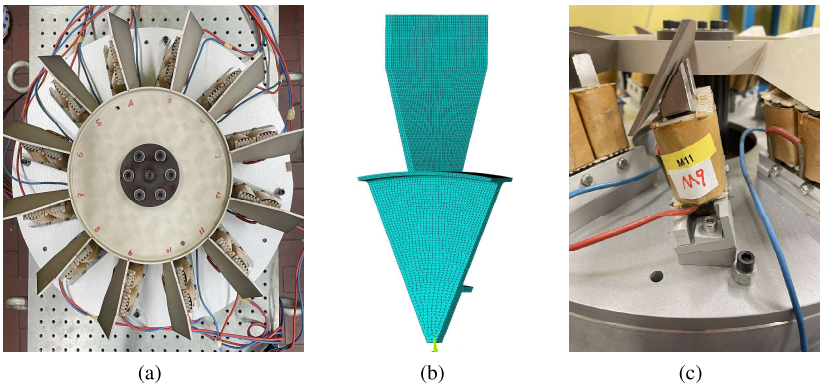

Fig. 1 Simplified blisk test piece mounted on a traveling wave excitation test rig: (a) blisk structure; (b) nominal sector model; (c) an electromagnetic unit.

strength. This research focuses on the 1st and 3rd mode family in Fig. 2, which correspond to the first bending (1B) and first torsional (1T) blade-dominated mode family, respectively. The 2nd mode family is not of interest because it is a typical disk-dominant family. From the CI values in Fig. 2, it can be inferred that the 1B mode family exhibits stronger inter-blade coupling than the 1T mode family does. This feature tends to confine more modal strain energy into the disk for the 1B mode family. It has been demonstrated [16], and it will be shown afterwards, that the inter-blade coupling is one of the critical factors that governs the performance of the already mentioned blade detuning tests.

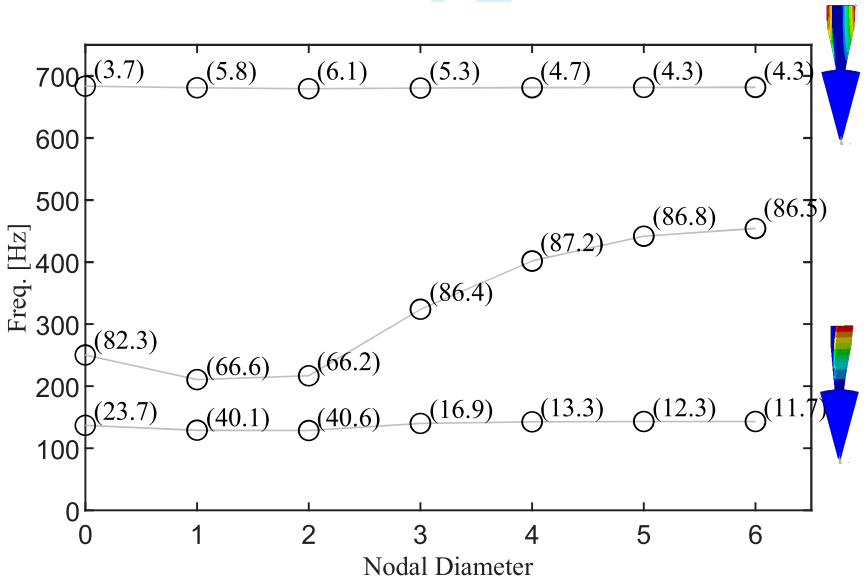

Fig. 2 Frequency vs nodal diameter diagram with Coupling indices in percentage.

Fig. 3 gives an overview of the various dynamic modeling approaches and test campaigns presented in this section. Modal test data including natural frequencies and full-blisk mode shapes are crucial for the conventional identification

methods. Depending on the ROM technique, blade mistuning can be identified either as $\boldsymbol{\delta}^{\mathrm{FMMID}}$ by FMMID, or $\boldsymbol{\delta}^{\mathrm{CMMID}}$ by CMMID. The experimentally derived blade mistuning will be injected into a tuned blisk model, leading to Model-FMMID and Model-CMMID for the blisk, respectively. By contrast, the BDTID method based on blade-by-blade detuning tests does not require the full-blisk modal tests. With the identified blade mistuning $\boldsymbol{\delta}^{\mathrm{BDTID}}$, Model-BDTID can be constructed in a similar manner.

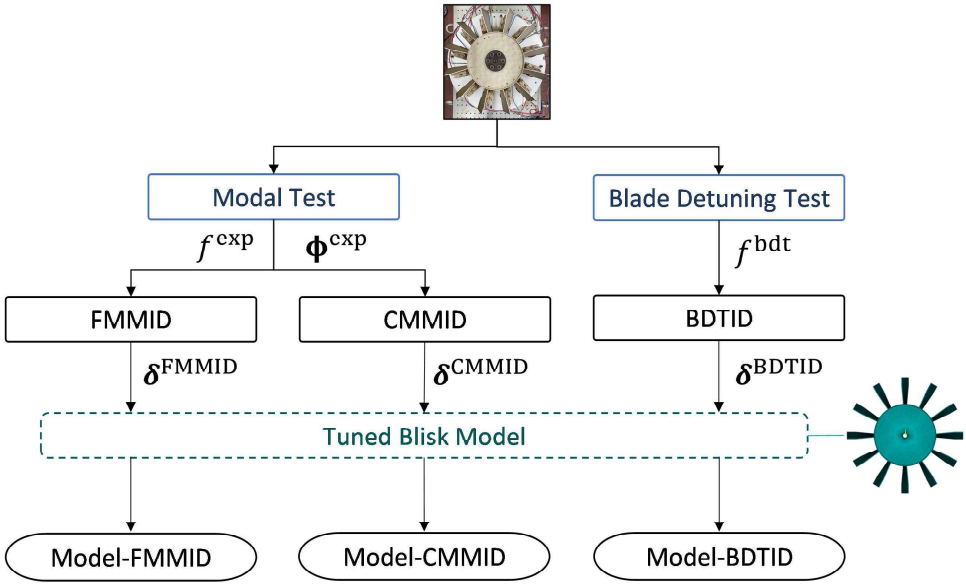

Fig. 3 Schematic diagram of the dynamic modeling approaches

A. Dynamic modeling based on conventional identification methods

The standard single-input modal test is briefly described before proceeding into the dynamic modeling methodologies based on the conventional identification procedures. The modal test setup is shown in Fig. 4. A miniature instrumented hammer is used to impulsively excite the blisk at the disk rim, in order to avoid double-hit. The vibration response is measured by the non-contact Laser Doppler vibrometer (LDV) at a tip point of each individual blade. The hammer force and LDV velocity are acquired and processed by the Test.Lab software in order to obtain the Frequency Response Functions (FRFs). The mistuned blisk frequencies and one-point-per-blade mode shapes are extracted from the measured FRFs by employing the PolyMax algorithm.

It should be emphasized that performing a high-quality modal test is essential to ensure sufficient accuracy for the FMMID and CMMID procedures. However, the test campaign is often cumbersome and technically difficult due to the fact that mistuned blisks are lightly damped structures with several modes occurring in a very narrow frequency band. In the test practice, some precautions must be taken in order to capture the mistuned blisk mode shapes as accurate as possible [8]: (I) the frequency resolution of the measured FRFs should be sufficient to extract the two split modes with

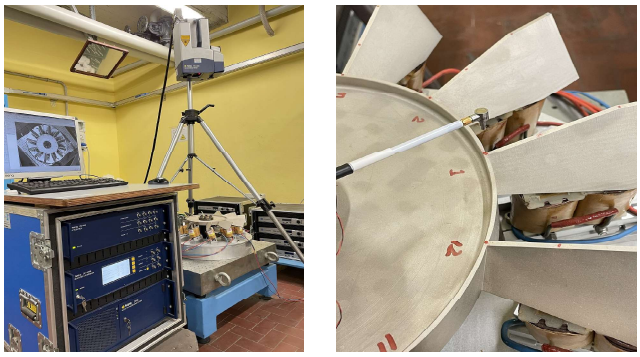

(a) (b)

Fig. 4 Modal test for the clamped blisk: (a) test setup; (b) impulsive excitation point.

closely spaced frequencies, rather than as a single mode; (II) the impulsive excitation point in the single-input modal test should be well selected so that the mistuned blisk modes, particularly the localized ones, could be fully excited and extracted; (III) the impulsive excitation point should be fixed during the modal test in order to avoid distortion in the extracted blisk mode shapes.

In this research, all the mistuned blisk modes ($N = 12$ modes associated with the target 1B and 1T mode family, respectively) are successfully extracted from the modal test FRFs. They provide experimental inputs to embark on the FMMID and CMMID procedures, which are presented in the forthcoming paragraphs. Moreover they will also serve as experimental reference data for the validation of the different models in Sec. III.

1. Model-FMMID

The FMMID method is derived from the well-known Fundamental Mistuning Model (FMM), which is a highly efficient reduced-order model specifically developed for a bladed disk with an isolated family of modes. FMM assumes the bladed disk is mistuned by small sector frequency variations, and that the mistuned system modes can be captured by a subset of tuned system modes. Provided the tuned system frequencies in a diagonal matrix $\mathbf{\Omega}^\circ$, the tuned system modes in the modal matrix $\mathbf{\Phi}^\circ$, and a matrix of the Discrete Fourier Transforms (DFT) of the sector frequency deviation $\bar{\mathbf{\Omega}}$ as known quantities, the dynamic characteristics of a mistuned bladed disk can be predicted by the FMM equation [3]:

$$(\mathbf{\Omega}^{\circ 2} + 2\mathbf{\Omega}^\circ \bar{\mathbf{\Omega}} \mathbf{\Omega}^\circ)\boldsymbol{\beta}_j = \omega_j^2 \boldsymbol{\beta}_j \tag{1}$$

where ω_j is the j^{th} mistuned system frequency, $\boldsymbol{\beta}_j$ is a vector of weighting factors that interprets the j^{th} mistuned mode $\boldsymbol{\phi}_j$ as a linear sum of the tuned system modes, i.e. $\boldsymbol{\phi}_j = \mathbf{\Phi}^\circ \boldsymbol{\beta}_j$. FMM is featured by a minimal input requirement. Its application is restricted to the blade-dominant mode family with closely spaced natural frequencies.

FMMID exploits the inversion of FMM equation and takes the experimentally derived mistuned mode $\boldsymbol{\phi}_j^{\text{exp}}$

(accordingly $\boldsymbol{\beta}_j^{\text{exp}}$) and frequencies ω_j^{exp} as known quantities. Eq. 1 can be reshaped by some algebraic manipulations as follows:

$$\begin{bmatrix} \mathbf{B}_j & 2\boldsymbol{\Omega}^{\circ}\boldsymbol{\Gamma}_j \end{bmatrix} \begin{bmatrix} \boldsymbol{\lambda} \\ \bar{\boldsymbol{\omega}} \end{bmatrix} = (\omega_j^{\text{exp}})^2 \boldsymbol{\beta}_j^{\text{exp}} \tag{2}$$

where $\mathbf{B}_j$ is a matrix composed of the elements of $\boldsymbol{\beta}_j^{\text{exp}}$, the matrix $\boldsymbol{\Gamma}_j$ contains the elements that are the product of $\boldsymbol{\Omega}^{\circ}$ and $\boldsymbol{\beta}_j^{\text{exp}}$. $\boldsymbol{\lambda}$ represents a vector of the tuned system frequencies and $\bar{\boldsymbol{\omega}}$ stands for the vector of DFT of the sector frequency deviations.

With the measured modal information of the j^{th} mode, FMMID allows the simultaneous identification of the tuned system frequencies and sector frequency deviations by solving Eq. 2 for the unknown vector $[\boldsymbol{\lambda}, \bar{\boldsymbol{\omega}}]^{\text{T}}$. In the practical implementation, several measurements of mistuned modes are incorporated into Eq. 2 for the purpose of mitigating the identification errors from measured variations. The problem of blade mistuning identification is then converted into finding a least-squares solution in an iterative way, which gives the best fit to the multiple measured mistuned modes.

As a last step, the tuned system frequencies and sector frequency deviations from FMMID are injected into the FMM reduced-order model represented by Eq. 1, leading to the final Model-FMMID. In addition, the equivalent blade frequency mistuning patterns ${}^{f}\boldsymbol{\delta}^{\text{FMMID}}$ can be deduced from the computed sector frequency deviations $\bar{\boldsymbol{\omega}}$, where the preceding superscript ${}^{f}(\cdot)$ stands for the blade frequency mistuning pattern in this paper. They will be graphically presented later on in Sec. III.D for the comparison purpose.

2. Model-CMMID

The CMMID method relies on the Component Mode Mistuning (CMM) reduced-order modeling technique for small blade stiffness mistuning. Similar to the FMM, the CMM formulation starts from the projection of the mistuned system mode $\boldsymbol{\phi}$ onto a set of retained tuned system modes $\boldsymbol{\Phi}^{\circ}$:

$$\boldsymbol{\phi} = \boldsymbol{\Phi}^{\circ}\mathbf{p} \tag{3}$$

where $\mathbf{p}$ is a vector of modal coordinates.

In the derivation of the CMM formulation, blade stiffness mistuning is projected to the N_{cb} cantilevered-blade normal modes. The contribution of each cantilevered-blade normal mode is quantified by the modal participation factors in the matrix $\mathbf{Q}$. The governing CMM equation of the dynamic characteristics reads [4]:

$$\left[-\omega^2\mathbf{I} + \left(\boldsymbol{\Omega}^{\circ} + \mathbf{Q}^{\text{T}}\boldsymbol{\kappa}^{\delta}\mathbf{Q}\right)\right]\mathbf{p} = \mathbf{0} \tag{4}$$

where $\boldsymbol{\kappa}^{\delta}$ is a diagonally dominant matrix, whose diagonal elements represents the cantilevered-blade eigenvalue

deviations.

For the purpose of blade mistuning identification, the modal coordinates $\mathbf{p}_j^{\text{exp}}$ (with $j = 1, 2, \cdots, N_m$) can be estimated from the N_m measured full-blisk mode shapes according to Eq. 3. Note that the computation of the tuned system frequencies $\mathbf{\Omega}^\circ$ and modes $\mathbf{\Phi}^\circ$, as well as the modal participation factors $\mathbf{Q}$ is carried out on the ideal tuned blisk model. The concept of 'cyclic modeling error' has been therefore proposed, which refers to the inevitable discrepancy between the ideal tuned blisk model and the virtual, underlying tuned system associated with the blisk structure. It is pointed out that the cyclic modeling error might deteriorate the identification accuracy. Hence, CMMID tends to consider both the tuned system frequencies in a vector of $\boldsymbol{\lambda}$ and blade mistuning in the form of cantilevered-blade eigenvalue deviations $\boldsymbol{\lambda}_j^{\delta,\text{cb}}$ (where $j = 1, 2, \cdots, N$) as the unknown quantities to be identified. Eq. 4 is therefore transformed into the following set of linear equations:

$$\begin{bmatrix} \mathbf{L}_2\mathbf{p}_1^{\text{exp}} & \mathbf{L}_3\mathbf{p}_1^{\text{exp}} & \cdots & \mathbf{L}_N\mathbf{p}_1^{\text{exp}} & \text{diag}(\mathbf{p}_1^{\text{exp}}) \\ \mathbf{L}_2\mathbf{p}_2^{\text{exp}} & \mathbf{L}_3\mathbf{p}_2^{\text{exp}} & \cdots & \mathbf{L}_N\mathbf{p}_2^{\text{exp}} & \text{diag}(\mathbf{p}_2^{\text{exp}}) \\ \vdots & \vdots & \ddots & \vdots & \vdots \\ \mathbf{L}_2\mathbf{p}_{N_m}^{\text{exp}} & \mathbf{L}_3\mathbf{p}_{N_m}^{\text{exp}} & \cdots & \mathbf{L}_N\mathbf{p}_{N_m}^{\text{exp}} & \text{diag}(\mathbf{p}_{N_m}^{\text{exp}}) \end{bmatrix} \begin{bmatrix} \lambda_2^{\delta,\text{cb}} \\ \vdots \\ \lambda_N^{\delta,\text{cb}} \\ \boldsymbol{\lambda} \end{bmatrix} = \begin{bmatrix} \omega_1^2\mathbf{p}_1^{\text{exp}} \\ \omega_2^2\mathbf{p}_2^{\text{exp}} \\ \vdots \\ \omega_{N_m}^2\mathbf{p}_{N_m}^{\text{exp}} \end{bmatrix} \tag{5}$$

with

$$\mathbf{L}_j = \mathbf{Q}_j^{\text{T}}\mathbf{Q}_j - \mathbf{Q}_1^{\text{T}}\mathbf{Q}_1 \tag{6}$$

where $\mathbf{Q}_j$ is the jth row of the matrix $\mathbf{Q}$, $\text{diag}(\mathbf{p}_j^{\text{exp}})$ denotes a diagonal matrix with the elements of vector $\mathbf{p}_j^{\text{exp}}$ on the main diagonal. Note that $\lambda_1^{\delta,\text{cb}}$ is purposefully eliminated in Eq. 5. Accordingly, the mean value of the cantilevered-blade eigenvalue deviations becomes zero and arbitrariness of the identified blade mistuning pattern can be removed.

CMMID enables to simultaneously identify the tuned system frequencies and blade mistuning by solving Eq. 6. The identified tuned system frequencies are then used to update the CMM reduced-order model of Eq. 4 such that the cyclic modeling error is compensated. Furthermore, Model-CMMID is generated by injecting the identified blade-alone mistuning patterns into the updated CMM reduced-order model.

B. Dynamic modeling based on BDTID

The BDTID method will be firstly reviewed and special attention is paid to its performance under different blade detuning test quality.

1. BDTID method

The BDTID method starts from blade detuning tests, which allow to approximately evaluate the 'blade-alone' frequencies through blade-by-blade measurements. As shown in Fig. 5a, the detuning mechanism is realized by attaching

identical detuning mass (2 squared magnets with a total weight $2m^{\mathrm{d}} = 3.5\mathrm{g}$) onto all the blades at the same position, except the one currently under test. The detuning mass position is optimized such that it covers the surface area with the maximum kinetic energy density in the target 1B and 1T blade mode. This usually leads to a good blade mode decoupling performance during the blade detuning test.

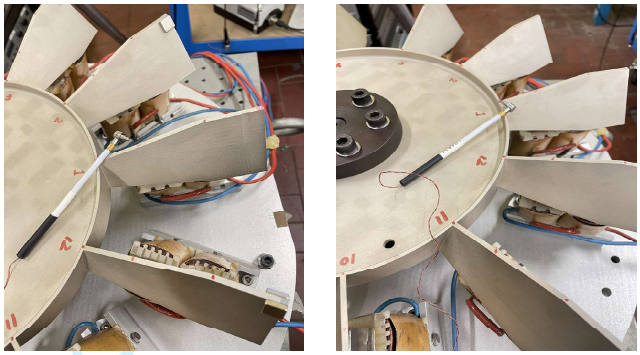

(a) (b)

Fig. 5 (a) Blade detuning test with 2 squared detuninng masses; (b) conventional blade test.

The blade detuning test is an impact test consisting in an impulsive excitation of the blade without detuning mass and meanwhile the response measurement at the blade tip. This results in a single BDT FRF for each individual blade, as depicted in Fig. 6. For the sake of comparison, the FRF generated by the impact test for the same blade but in the blisk without any detuning mass, is also included (see Fig. 5b) and denoted as 'CBT' (conventional blade test). The CBT FRFs are characterized by clustered peaks due to high modal density and blade mistuning effect. In contrast, the BDT FRF around the 1B mode family in Fig. 6a exhibits a global drift with respect to the CBT FRF and an isolated peak with the highest magnitude is manifested. This is referred as blade mode decoupling phenomenon, since at this peak frequency the individual blade's modal vibration is largely decoupled from the whole blisk. The peak frequency $f^{\mathrm{bdt}}_{m,j}$ or $\omega^{\mathrm{bdt}}_{m,j}$ is therefore taken as an approximated m-th blade-alone modal frequency of the j-th blade. A better decoupling performance is achieved for the 1T mode in Fig. 6b. Only a single well-isolated peak is clearly visible in the BDT FRF, which indicates that it appears as a pure 1T blade-alone mode.

The blade detuning test is repeated for all the blades one by one. It allows to straightforwardly evaluate the m-th 'blade-alone' frequency mistuning pattern as ${}^{f}\boldsymbol{\delta}^{\mathrm{bdt}}_{m} = [{}^{f}\delta^{\mathrm{bdt}}_{m,1}, \cdots, {}^{f}\delta^{\mathrm{bdt}}_{m,N}]^{\mathrm{T}}$

$$ {}^{f}\delta^{\mathrm{bdt}}_{m,j} = \frac{f^{\mathrm{bdt}}_{m,j}}{\bar{f}^{\mathrm{bdt}}_{m}} - 1 \tag{7} $$

or equivalently ${}^{E}\delta^{\mathrm{bdt}}_{m,j} \approx 2{}^{f}\delta^{\mathrm{bdt}}_{m,j} + ({}^{f}\delta^{\mathrm{bdt}}_{m,j})^2$ in terms of the variation of blade's elastic modulus. $\bar{f}^{\mathrm{bdt}}_{m}$ is the mean value of the m-th blade-alone modal frequencies extracted from the blade detuning tests for all the N blades.

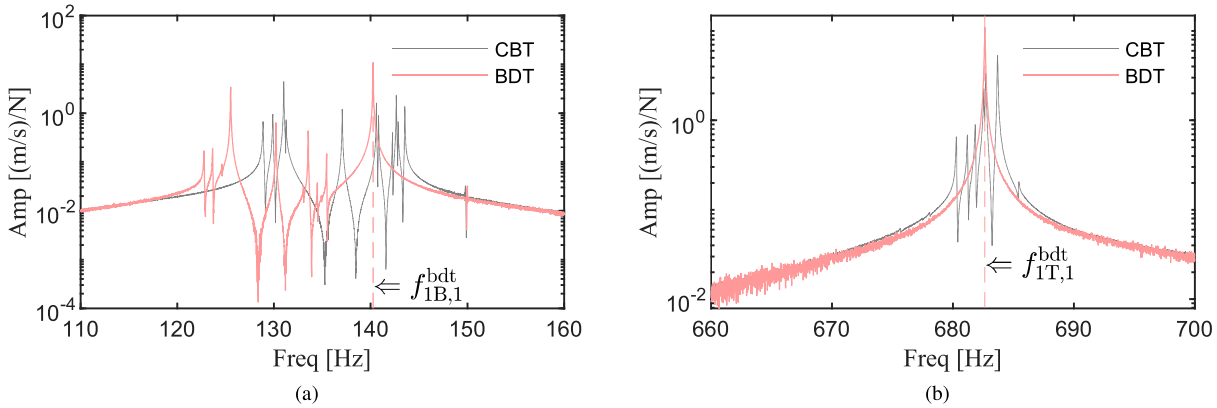

Fig. 6 Comparison of test FRFs at blade 1: (a) around 1B mode family; (b) around 1T mode family.

Subsequently, the BDTID method applies a correction procedure to account for the residual inter-blade coupling in the presence of detuning masses, which is responsible for the potentially inaccurate blade mistuning evaluation by Eq. 7. The correction procedure is established based on the following compact formulation:[16]:

$$\frac{{\omega^{\text{bdt}}_{m,j}}^2 - \omega^2_{\text{ref}}}{\omega^2_{\text{ref}}} = \boldsymbol{\psi}^{\text{T}} \cdot {}^{E}_{\text{ref}}\boldsymbol{\delta}_m \tag{8}$$

The left-hand side of Eq. 8 denotes the variation of the isolated peak frequency ${\omega^{\text{bdt}}_{m,j}}^2$ of blade j in the blade detuning test with respect to a reference frequency ω^2_{ref}. ${}^{E}_{\text{ref}}\boldsymbol{\delta}_m$ is the 'true' blade modulus mistuning pattern to be determined for the m-th blade mode. The preceding subscript ${}_{\text{ref}}(\cdot)$ implies that its reference should be consistent with ω_{ref}. $\boldsymbol{\psi} = [\psi_l, \ldots, \psi_{-1}, \psi_0, \psi_1, \ldots, \psi_u]^{\text{T}}$ is a vector of influence coefficients, which quantitatively measure the residual inter-blade coupling, i.e., the influence of one blade's vibration on all the other blades with detuning masses. Note that its entries are always centered around the j-th blade in order to account for its cyclic nature. Specifically, the j-th entry of $\boldsymbol{\psi}$ is set as ψ_0, meanwhile ψ_{-1} and ψ_1 stand for the influence coefficients of the nearest neighboring blades to the j-th one, etc. An important remark is that ψ_0 can be seen as an indicator of the residual inter-blade coupling strength, and accordingly, adequacy of blade vibration isolation during the BDT. In an ideal case where the detuning mass perfectly isolates the blades from one another, i.e., no residual coupling remains among the blades, $\boldsymbol{\psi}$ will have all zeros except for ψ_0=1.

An important remark is that apart from the adequacy of the mass detuning mechanism, the influence coefficients $\boldsymbol{\psi}$ in Eq. 8 also show partial dependence on the intrinsic blade mistuning pattern ${}^{E}_{\text{ref}}\boldsymbol{\delta}_m$. On the contrary, a similar formulation established in the previous research [14] assumes that the influence coefficients are independent from the blade mistuning pattern. Relying on different assumptions, the correction procedure implemented as a two-step scheme